Depositional environments of Lower Cretaceous (Ryazanian–Barremian) sediments from Wollaston Forland and Kuhn Ø, North-East Greenland

SEBASTIAN PAULY, JÖRG MUTTERLOSE & PETER ALSEN

Pauly, S., Mutterlose, J. & Alsen, P., 2013. Depositional environments of Lower Cretaceous (Ryazanian–Barremian) sediments from Wollaston Forland and Kuhn Ø, North-East Greenland. ©2013 by Bulletin of the Geological Society of Denmark, Vol. 61, pp. 19–36. ISSN 2245-7070. (www.2dgf.dk/publikationer/bulletin). https://doi.org/10.37570/bgsd-2013-61-02

Lower Cretaceous sediments from the Wollaston Forland–Kuhn Ø area in North-East Greenland have been analyzed for stable carbon isotopes, total organic carbon (TOC) content, and major and trace elements, aiming at a lithological characterization and reconstruction of the depositional environments. The marine sediments of Ryazanian–Barremian age were deposited in North-East Greenland directly after a major Late Jurassic – earliest Cretaceous rifting event. The Lower Cretaceous post-rift sediments are composed of fossiliferous calcareous mud- and marlstones assigned to the Albrechts Bugt (upper Ryazanian – Valanginian) and Rødryggen (Hauterivian) Members. The calcareous sediments are commonly sandwiched between black mudstones of Late Jurassic – earliest Cretaceous (Bernbjerg Formation) and mid Cretaceous (unnamed formation) age. The carbon isotope curves present the first record for the Lower Cretaceous (upper Ryazanian – Barremian) of North-East Greenland. The Ryazanian – Hauterivian sediments are characterized by a mixture of terrigenous detrital matter (quartz, clay minerals, heavy minerals) similar to average shale, with varying $CaCO_3$ concentrations. The Barremian black mudstones on the contrary have lower $CaCO_3$ and higher clay mineral contents. The deposition of the Bernbjerg Formation took place under anoxic bottom water conditions. The depositional environment of the Albrechts Bugt and Rødryggen Members is characterized by well-oxygenated sea-floor conditions, hemipelagic sedimentation of fine-grained terrigeneous detrital matter, and biogenic carbonate settling. After this relatively short interval of carbonate sedimentation under oxic conditions, bottom waters were affected by dysoxic conditions, responsible for the burial of organic matter in the Barremian.

Keywords: Carbon isotope record, TOC, sediment geochemistry, North-East Greenland, Bernbjerg Formation, Albrechts Bugt Member, Rødryggen Member, depositional environment.

Sebastian Pauly [sebastian.pauly@rub.de], Jörg Mutterlose [joerg.mutterlose@rub.de], Institute of Geology, Mineralogy and Geophysics, Ruhr-University Bochum, Universitätsstrasse 150, D-44801, Germany. Peter Alsen [pal@geus.dk], Geological Survey of Denmark and Greenland (GEUS), Øster Voldgade 10, DK-1350 Copenhagen K, Denmark.

Received 28 May 2012
Accepted in revised form
25 June 2013
Published online
23 August 2013

The Greenland–Norwegian Seaway is an important area for understanding the Early Cretaceous palaeoclimate and palaeoceanography. Marine sediments of Early Cretaceous age occur both in North-East Greenland (e.g. Alsen 2006; Pauly *et al*. 2012a) and along the shelf area of Norway and in the Barents Sea (Mutterlose *et al*. 2003). New assessments of undiscovered oil and gas resources suggest that North-East Greenland will form a significant future petroleum province. The potential for the Mesozoic rift basin sediments to serve as a source and a reservoir rock for hydrocarbon explain the intensification of the geological and palaeontological investigations in North-East Greenland.

Important sedimentological and stratigraphic studies of the Jurassic–Cretaceous successions of North-East Greenland were undertaken by Surlyk *et al*. (1973), Surlyk & Clemmensen (1975a,b) and Surlyk (1978, 1984, 2003). Nøhr-Hansen (1993) examined the dinoflagellate cyst stratigraphy of Early Cretaceous successions. Alsen & Rawson (2005) and Alsen (2006) investigated the Lower Cretaceous ammonite faunas, palaeobiogeographical aspects of Early Cretaceous brachiopods were covered by Harper *et al*. (2005), and belemnites by Alsen & Mutterlose (2009). Most recent publications deal with the integrated stratigraphy and palaeoecology of Lower Cretaceous sediments from

Wollaston Forland and Kuhn Ø (Pauly *et al*. 2012a,b). The accumulation of the high latitudinal calcareous sediments is related to an important influx of calcareous nannofossils into the Greenland–Norwegian Seaway. The unusually well-preserved calcareous nannofossil assemblages exhibit an influx of Tethyan and low-to-mid latitudinal taxa, synchronous with observed influxes of Tethyan ammonite and belemnite species (Alsen 2006; Alsen & Mutterlose 2009). These influxes suggest the occurrence of northward flowing surface currents, which allowed Tethyan nekton and plankton to spread as far north as North-East Greenland (55°N palaeolatitude). Further fluctuations in the composition of calcareous nannofossil assemblages indicate a general cooling trend for the late Ryazanian – Valanginian and a subsequent change to warmer climatic conditions in the Hauterivian–Barremian (Pauly *et al*. 2012b).

This study aims at the lithological characterization of black mudstones and marlstones of Early Cretaceous age from Wollaston Forland and Kuhn Ø. Further it is intended to reconstruct the depositional environment on the basis of the total organic matter (TOC) and major and trace element concentrations. For a further characterization of the sedimentary units and detection of possible diagenetic alteration, stable carbon isotope records ($\delta^{13}C_{org}$ and $\delta^{13}C_{carb}$) are presented.

Geological setting and stratigraphy

The Upper Jurassic – Lower Cretaceous sedimentary succession in North-East Greenland reflects deposition during different stages of rifting between Greenland and Norway, related to the opening of the North Atlantic. The up to 3000 m thick sedimentary successions are characterized by coarse clastic sediments that accumulated in submarine fans along fault scarps in westward-tilted half-grabens (Surlyk 1978, 2003). The half-grabens were flooded in the middle Jurassic, reflected by marine deposits resting on Permian rocks or crystalline basement (Surlyk 1978, 2003). A maximum sea-level rise occurred in the Oxfordian to early Volgian, expressed by black mudstones assigned to the Bernbjerg Formation (Surlyk 1990). The rift climax in the middle Volgian to late Ryazanian led to basin infill by coarse clastic deposits, which were draped by thin late Ryazanian – Hauterivian marine deposits at the end and shortly after the major rifting event (Surlyk 1978). These late Ryazanian – Hauterivian sediments are characterized by fossiliferous, calcareous nannofossil bearing mud- and marlstones assigned to the Albrechts Bugt and Rødryggen Members (Palnatokes Bjerg Formation). Integrated calcareous nannofossil and ammonite data from the Wollaston Forland–Kuhn Ø area (Fig. 1) allow a biostratigraphic zonation scheme for the Early Cretaceous Boreal-Arctic Province of the Boreal Realm which give a precise age for the first time. At the studied sections, the 22–34 m thick Albrechts Bugt Member is assigned to the Boreal calcareous nannofossil zones BC 1–5 (upper Ryazanian to Valanginian), and the 3.5–5 m thick Rødryggen Member to zones BC6–11 (Hauterivian) (Pauly *et al*. 2012a). The calcareous sediments are commonly sandwiched within a kilometre-thick mid Jurassic to mid Cretaceous black mudstone succession.

Material and methods

Sections

Rødryggen: The Rødryggen section is situated in the central northern part of Wollaston Forland (Fig. 1) on the western shoulder of a ridge (74°32′47.1″N, 19°50′35.5″W, 65 m a.s.l.), spanning the upper Ryazanian (BC1 Zone) to Hauterivian/Barremian boundary (BC11 Zone) (Pauly *et al*. 2012a). The Albrechts Bugt and Rødryggen Members are here under- and overlain by black mudstones of Ryazanian (Bernbjerg Formation) and Barremian age respectively. The Albrechts Bugt (22 m thick) and Rødryggen members (5 m thick) are composed of calcareous mudstones. A total of 150 rock samples were collected at 20 cm intervals from the Bernbjerg Formation, Albrechts Bugt and Rødryggen Members, and the Barremian (unnamed formation).

Perisphinctes Ravine: At the east coast of Kuhn Ø (74°48′07.1″N, 19°52′56.2″W, 124 m a.s.l.) (Fig. 1) the upper Ryazanian – Valanginian Albrechts Bugt Member and Hauterivian Rødryggen Member are exposed on a steep slope in a ravine, spanning the upper Ryazanian (BC1 Zone) to Hauterivian/Barremian boundary (BC11 Zone) (Pauly *et al*. 2012a). Both units are sandwiched by Ryazanian and Barremian black mudstones. The Albrechts Bugt (34 m thick) and Rødryggen Members (3.5 m thick) consist of calcareous mudstones. A total of 140 rock sediment samples were collected at 25 cm intervals from the Bernbjerg Formation, Albrechts Bugt and Rødryggen Members.

Carbon and oxygen isotope analyses ($\delta^{13}C_{carb}$, $\delta^{18}O_{carb}$ and $\delta^{13}C_{org}$)

Carbon and oxygen isotope analysis of bulk-rock samples was performed on 102 samples with >6% $CaCO_3$ (49 from the Rødryggen section, 53 from the Perisphinctes Ravine section) for the upper Ryaza-

nian – Hauterivian, using a Finnigan MAT 251 mass spectrometer, coupled to the Carbo Kiel device at the Leibniz-Laboratory for Radiometric Dating and Stable Isotope Research in Kiel. The measurements yielded a precision of 0.06‰ for carbon and 0.07‰ for oxygen isotopes. Carbon isotope analysis of organic carbon was performed on 119 samples (70 from the Rødryggen section, 49 from the Perisphinctes Ravine section) for the lower Ryazanian – Barremian. Samples with a minimum of 0.02% TOC have been decarbonised on a hot plate (60°C) using 10% HCl and measured with an elemental analyser (Carlo-Erba 1110) connected online to a ThermoFinnigan Delta Plus mass spectrometer at the GeoZentrum Nordbayern, Erlangen. Reproducibility was better than ± 0.08‰ (1σ). All isotope values are reported in the conventional δ-notation in per mil relative to V-PDB (Vienna-PDB).

Total organic carbon, major and trace element analysis

Total organic carbon (TOC) analysis was performed on 88 samples (63 from the Rødryggen section, 25 from the Perisphinctes Ravine section) with a Deltatronik coulometer at the Ruhr-University Bochum, Germany. TOC was calculated as the difference between total carbon (TC) and total inorganic carbon (TIC): TOC=TC–TIC.

X-ray fluorescence (XRF) analysis for major and trace elements was carried out on 86 samples (62 from the Rødryggen section, 24 from the Perisphinctes Ravine section) with a Philips® PW 2400 X-ray spectrometer at the Department of Microbiogeochemistry, University of Oldenburg. An amount of 600 mg sample powder was mixed with 3600 mg of a 1:1 mixture of dilithium-tetraborate ($Li_2B_4O_7$) and lithium-metaborate ($LiBO_2$), or with 100% dilithium-tetraborate for carbonate-rich samples, pre-oxidized at 500°C with NH_4NO_3 (p.a.) and fused to glass beads.

Results

Carbon isotopes

The $\delta^{13}C_{carb}$ record is characterized by major variations (-11.1 to -0.3‰) in both sections (Fig. 2; Tables 1, 2). The samples show a distinctive ^{13}C depletion resulting in light $\delta^{13}C_{carb}$ values averaging -4.8‰ (Rødryggen section) and -3.8‰ (Perisphinctes Ravine section). The $\delta^{18}O_{carb}$ values are not presented due to the observed diagenetic overprint.

$\delta^{13}C_{org}$ values of the ***Rødryggen section*** range between -28.2 and -20.9‰ (Fig. 2).

Bernbjerg Formation (0–19 m, 5 samples): $\delta^{13}C_{org}$ values show a relatively stable development around -27.8‰.

Albrechts Bugt Member (19–41 m, 28 samples): Isotope ratios vary between -26.0 and -23.9‰ (average -25‰) in the Ryazanian interval, followed by an increase to -20.9‰ and a shift to -26.1‰ in the lower Valanginian interval. In the upper Valanginian interval, after a sample gap, $\delta^{13}C_{org}$ values stay relatively constant around -23‰ and increase to values around -25‰ at the top.

Rødryggen Member (41–46 m, 6 samples): $\delta^{13}C_{org}$ values are relatively constant around -25‰.

Barremian (46–77 m, 31 samples): Carbon isotope values show minor variations around -25‰ in the lower part (46–60 m) and -24‰ in the upper part (60–77 m).

$\delta^{13}C_{org}$ values of the ***Perisphinctes Ravine section*** vary between -27.7 and -22.5‰.

Bernbjerg Formation (0–4 m, 2 samples): $\delta^{13}C_{org}$ is relatively stable showing values around -27.6‰.

Albrechts Bugt Member (4–38 m, 39 samples): In the Ryazanian – lower Valanginian interval $\delta^{13}C_{org}$ values range between -25.6 and -24.2‰ (average -25‰). The upper Valanginian $\delta^{13}C_{org}$ record continues the previous trend before it marks a shift to lighter values (-27‰), followed by a shift to -25‰.

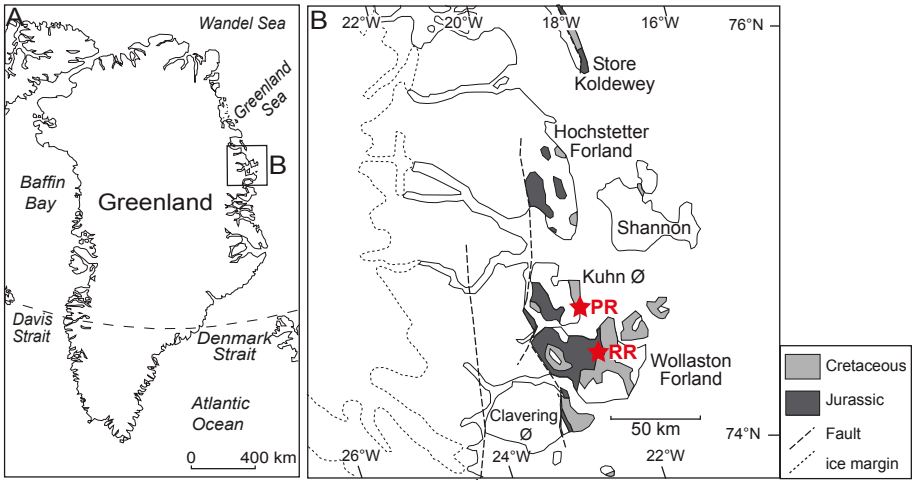

Fig. 1. Maps showing the location of the studied sections in North-East Greenland. **A:** Greenland. **B:** North-East Greenland (74°–76°N), showing the Wollaston Forland–Kuhn Ø area; RR: Rødryggen section; PR: Perisphinctes Ravine section (modified after Alsen 2006).

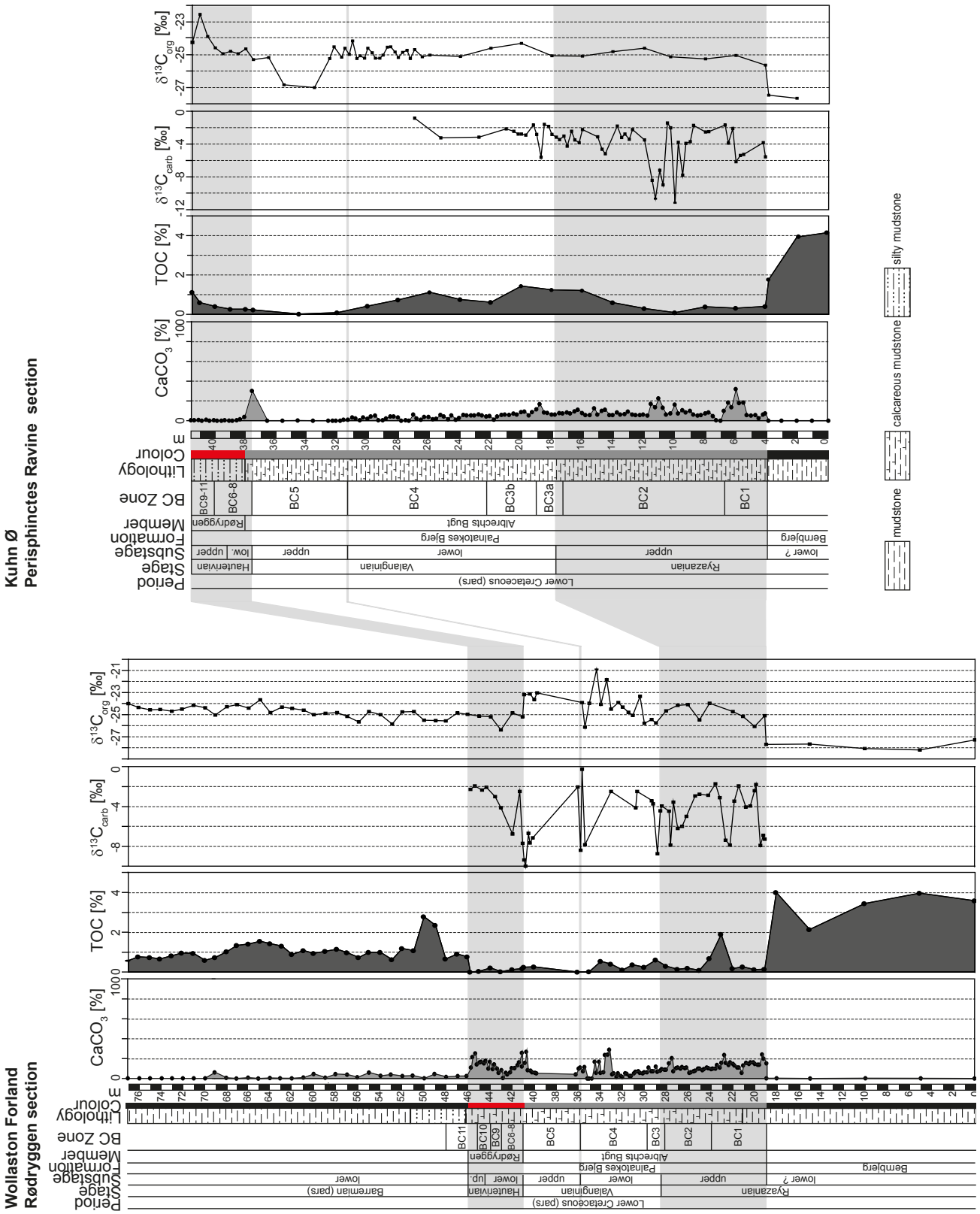

Fig. 2. Lithological logs of the Rødryggen and Perisphinctes Ravine sections showing the calcium carbonate (after Pauly *et al.* 2012b) and TOC contents and carbon isotope records ($\delta^{13}C_{carb}$, $\delta^{13}C_{org}$).

Table 1. $CaCO_3$ (from Pauly *et al*. 2012b) and TOC contents, $\delta^{13}C_{carb}$ and $\delta^{13}C_{org}$ values of the Rødryggen section (Wollaston Forland)

Sample no.	m	$CaCO_3$ [%]	TOC [%]	$\delta^{13}C_{carb}$ [‰]	±s	$\delta^{18}O_{carb}$ [‰]	±s	$\delta^{13}C_{org}$ [‰]
469521	77	2.3	0.6					-23.99
469520	76	0.5	0.8					-24.32
469519	75	2.8	0.7					-24.56
469518	74	0.3	0.7					-24.51
469517	73	4.1	0.8					-24.66
469516	72	0.1	1.0					-24.50
469515	71	0.2	0.9					-24.13
469514	70	2.5	0.6					-24.36
469513	69	6.2	0.7	-7.92	0.02	-10.34	0.02	-25.01
469512	68	0.7	1.0					-24.28
469511	67	0.1	1.4					-24.09
469510	66	0.8	1.4					-24.38
469509	65	0.1	1.6					-23.64
469508	64	0.5	1.4					-24.79
469507	63	0.2	1.3					-24.31
469506	62	0.2	0.9					-24.43
469505	61	1.0	1.1					-24.59
469504	60	4.6	1.0					-24.99
469503	59	0.8	1.1					-24.87
469502	58	4.5	1.2					-24.80
469501	57	3.9	1.0					-25.13
469500	56	1.3	0.7					-25.65
469499	55	6.0	1.0					-24.70
469498	54	2.8	1.0					-25.00
469497	53	4.0	0.6					-25.83
469496	52	2.5	1.2					-24.73
469495	51	2.9	1.1					-24.71
469494	50	0.2	2.8					-25.49
469493	49	4.6	2.4					-25.53
469492	48	1.6	0.7					-25.55
469491	47	2.4	0.9					-24.82
469490	46.1	2.5	0.8					-24.96
469489	45.8	11.1	0.0	-2.28	0.03	-4.40	0.03	
469488	45.6	21.6						
469487	45.4	25.3		-1.92	0.03	-3.61	0.03	
469486	45.2	14.2						
469485	45	16.3	0.0					-25.11
469484	44.8	16.8		-2.33	0.01	-5.89	0.01	
469483	44.6	15.3						
469482	44.4	17.9		-2.05	0.01	-5.00	0.02	
469481	44.2	10.0						
469480	44	16.8	0.2					-25.16
469479	43.8	9.5						
469478	43.6	14.2		-3.02	0.02	-2.10	0.01	
469477	43.4	10.0						
469476	43.2	5.8						
469475	43.0	8.4	0.0	-4.12	0.02	-3.88	0.01	-26.37
469474	42.8	0.5						
469473	42.6	5.8						
469472	42.4	4.2						
469471	42.2	6.3						
469470	42	10.5	0.1	-6.75	0.02	-5.44	0.03	-24.84
469469	41.8	10.5						
469468	41.6	13.4						
469467	41.4	16.3		-2.50	0.02	-5.25	0.01	
469466	41.2	25.8						
469465	41.1	12.1	0.2	-7.69	0.01	-6.14	0.01	-25.17
469464	40.9	15.8	0.3	-9.35	0.04	-7.35	0.05	-23.18
469463	40.8	26.8		-10.02	0.02	-6.42	0.05	
469462	40.6	8.4		-6.70	0.01	-7.75	0.01	
469461	40.4	7.9		-7.65	0.01	-8.06	0.02	-23.12
469460	40.2	6.3		-7.12	0.02	-7.66	0.02	
469459	40	5.8	0.3					-23.61
469458	39.8	5.3						-23.01
469457	36.2	4.2						
469456	36	10.0	0.0	-2.02	0.01	-8.66	0.02	
469455	35.8	11.1		-8.37	0.01	-5.98	0.03	
469454	35.6	7.4		-0.27	0.01	-8.25	0.02	-23.89
469453	35.4	11.6		-7.82	0.01	-6.80	0.03	-26.12
469452	35	0.0						
469451	35	0.0	0.0					-23.95
469450	35	0.0						
469449	34.6	16.8						
469448	34	5.8						-20.88
469447	34	16.8						
469446	34	5.8	0.5					-24.06
469445	34	6.3						
469444	34	23.7						
469443	33	24.2						-21.84
469442	33	29.0						
n		157	63	49		49		70

Sample no.	m	$CaCO_3$ [%]	TOC [%]	$\delta^{13}C_{carb}$ [‰]	±s	$\delta^{18}O_{carb}$ [‰]	±s	$\delta^{13}C_{org}$ [‰]
469441	33	4.3	0.4	-2.48	0.03	-5.49	0.04	-24.48
469440	32.8	5.3						
469439	33	1.6						
469438	32.4	5.3						-23.90
469437	32	2.6						
469436	32	1.4	0.1					-24.29
469435	32	5.3						
469434	31.6	4.7						
469433	31.4	2.6						-24.76
469432	31.2	2.6						
469431	31.0	5.3	0.4					-25.04
469430	31	6.8		-4.12	0.02	-6.67	0.03	
469429	30.6	7.4		-2.49	0.02	-5.51	0.02	
469428	30	5.8						-23.34
469427	30.2	5.3						
469426	30	6.3	0.3					-25.78
469425	29.8	6.3						
469424	29.6	11.1						
469423	29.4	7.4		-3.41	0.02	-5.88	0.03	-25.43
469422	29.2	7.4		-3.73	0.02	-5.30	0.01	
469421	29.0	12.0	0.6					-25.73
469420	28.8	6.8		-8.75	0.02	-10.08	0.05	
469419	28.6	7.9		-4.43	0.01	-3.93	0.03	
469418	28.4	9.5		-3.95	0.02	-4.76	0.02	
469417	28.2	9.0						
469416	28	9.0	0.3					-24.63
469415	27.8	15.3		-4.46	0.02	-5.15	0.02	
469414	27.6	20.5		-7.88	0.02	-6.73	0.02	
469413	27.4	7.4		-3.55	0.02	-5.33	0.02	
469412	27.2	10.5						
469411	27.0	11.1	0.1	-6.19	0.02	-4.90	0.01	-24.14
469410	26.8	10.0						
469409	26.6	11.6		-5.99	0.03	-4.91	0.03	
469408	26.4	10.5						
469407	26.2	11.1		-4.98	0.02	-4.17	0.04	
469406	26	5.8	0.2					-24.07
469405	25.8	6.3						
469404	25.6	7.4						
469403	25.4	7.9		-2.92	0.01	-5.05	0.03	
469402	25.2	10.0						
469401	25.0	10.0	0.1	-2.75	0.03	-5.19	0.02	-25.46
469399	24.8	8.4						
469398	24.6	9.5						
469397	24.4	11.1						
469396	24.2	10.5		-2.85	0.01	-4.54	0.02	
469395	24	9.5	0.7					-23.94
469394	23.8	10.0						
469393	23.6	10.0		-1.71	0.03	-4.71	0.03	
469392	23.4	13.7						
469391	23.2	11.1		-3.10	0.01	-4.56	0.01	
469390	23.0	15.8	1.9					
469389	22.8	23.7						
469388	22.6	15.8		-7.39	0.02	-5.55	0.02	
469387	22.4	13.7						
469386	22.2	16.3		-7.85	0.06	-4.84	0.07	
469385	22	14.7	0.2					-24.71
469384	21.8	13.2		-3.45	0.02	-5.54	0.03	
469383	21.6	11.1						
469382	21.4	11.1		-1.91	0.03	-5.99	0.03	
469381	21.2	5.8						
469380	21.0	13.2	0.3					-25.13
469379	20.8	15.8		-4.03	0.04	-5.61	0.04	
469378	20.6	14.7						
469377	20.4	16.3		-3.95	0.04	-6.06	0.05	
469376	20.2	16.3						
469375	20	14.7	0.1	-2.41	0.02	-4.48	0.04	-26.04
469374	19.8	13.9		-1.80	0.02	-5.56	0.02	
469373	19.6	13.9						
469372	19.4	24.2		-7.90	0.02	-8.21	0.03	
469371	19.2	20.0		-6.89	0.02	-7.40	0.03	
469370	19	15.3	0.2	-7.28	0.02	-6.90	0.04	-25.07
469369	18.9	0.2						-27.66
469368	18	0.0	4.0					
469365	15	0.0	2.1					-27.63
469360	10	0.0	3.5					-28.06
469355	5	0.0	4.0					-28.17
469351	0	0.0	3.6					-27.28
n		157	63	49		49		70

Table 2. $CaCO_3$ (from Pauly *et al*. 2012b) and TOC contents, $\delta^{13}C_{carb}$ and $\delta^{13}C_{org}$ values of the Perisphinctes Ravine section (Kuhn Ø)

Sample no.	m	$CaCO_3$ [%]	TOC [%]	$\delta^{13}C_{carb}$ [‰]	±s	$\delta^{18}O_{carb}$ [‰]	±s	$\delta^{13}C_{org}$ [‰]
518278	41.5	0.5	1.1					-24.24
518277	41.25	0.5						
518276	41	0.8	0.6					-22.53
518275	40.75	0.0						
518274	40.5	1.0						-23.89
518273	40.25	0.0						
518272	40	0.5	0.4					-24.57
518271	39.75	0.0						
518270	39.5	0.0						-24.94
518269	39.25	0.5						
518268	39	0.1	0.3					-24.80
518267	38.75	0.0						
518266	38.5	0.5						-24.93
518265	38.25	1.5						
518264	38	3.9	0.3					-24.64
518263	37.5	30.2	0.2					-25.30
518262	36.5	0.0						-25.17
518261	35.5	0.0						-26.83
518260	34.5	0.3	0.0					
518259	33.5	0.0						-26.99
518258	32.5	0.0						-25.24
518257	32.25	0.0						-24.51
518256	32	0.0	0.1					
518255	31.75	0.0						-25.14
518254	31.5	1.0						-24.61
518253	31.25	1.0						-24.97
518252	31	3.4						-24.16
518251	30.75	2.4						-25.23
518250	30.5	0.5						-25.06
518249	30.25	3.4						-25.22
518248	30	2.0	0.4					-24.61
518247	29.75	4.4						-24.87
518246	29.5	5.3						-25.20
518245	29.25	0.5						-25.20
518244	29	0.5						-25.03
518243	28.75	2.4						-24.54
518242	28.5	4.4						-24.51
518241	28.25	4.4						-24.83
518240	28	3.4	0.8					-25.16
518239	27.75	0.0						-24.85
518238	27.5	0.5						-24.73
518237	27.25	0.0						-25.23
518236	27	6.3		-0.80	0.00	-6.79	0.00	-24.69
518235	26.75	2.4						
518234	26.5	1.0						-25.12
518233	26.25	3.9						
518232	26	3.9	1.1					-25.02
518231	25.75	1.5						
518230	25.5	2.0						
518229	25.25	5.9		-3.22	0.01	-6.44	0.02	
518228	25	4.4						
518227	24.75	1.5						
518226	24.5	5.4						
518225	24.25	1.0						
518224	24	2.9	0.8					-25.11
518223	23.75	5.9						
518222	23.5	5.4						
518221	23.25	5.4						
518220	23	5.4						
518219	22.75	6.4		-3.12	0.00	-6.00	0.01	
518218	22.5	5.4						
518217	22.25	4.4						
518216	22	4.9	0.6					-24.61
518215	21.75	1.1						
518214	21.5	4.4						
518213	21.25	5.9						
518212	21	6.3		-2.12	0.01	-5.76	0.02	
518211	20.75	5.9						
518210	20.5	7.3		-2.44	0.01	-7.07	0.02	
518209	20.25	6.3		-2.77	0.00	-6.83	0.01	
518208	20	8.8	1.5	-2.76	0.01	-6.32	0.01	-24.30
518207	19.75	9.3		-2.90	0.00	-6.49	0.01	
518206	19.5	5.4						
518205	19.25	8.8		-1.66	0.01	-6.46	0.01	
518204	19	11.6		-2.82	0.00	-5.45	0.02	
518203	18.75	16.8		-5.60	0.01	-4.79	0.01	
518202	18.5	8.4		-1.57	0.00	-6.43	0.01	
518201	18.25	7.9		-1.85	0.01	-6.02	0.03	
518199	18	6.3	1.3	-2.79	0.00	-6.41	0.02	-25.07
n		140	25	53		53		49

Sample no.	m	$CaCO_3$ [%]	TOC [%]	$\delta^{13}C_{carb}$ [‰]	±s	$\delta^{18}O_{carb}$ [‰]	±s	$\delta^{13}C_{org}$ [‰]
518198	17.75	6.3		-3.13	0.00	-5.51	0.02	
518197	17.5	7.8		-3.42	0.00	-5.73	0.01	
518196	17.25	7.4		-3.02	0.01	-6.04	0.01	
518195	17	8.4		-4.23	0.00	-5.49	0.02	
518194	16.75	7.4		-2.44	0.00	-5.52	0.01	
518193	16.5	9.5		-3.47	0.01	-4.55	0.01	
518192	16.25	11.2		-3.83	0.00	-5.62	0.00	
518191	16	7.8	1.2	-2.22	0.01	-4.62	0.02	-25.09
518190	15.75	5.8						
518189	15.5	5.8						
518188	15.25	12.6						
518187	15	6.3		-3.08	0.00	-5.84	0.01	
518186	14.75	10.0		-4.62	0.01	-5.22	0.01	
518185	14.5	11.2		-5.15	0.01	-3.93	0.03	
518184	14.25	5.8						
518183	14	5.8	0.6					-24.82
518182	13.75	8.4		-1.78	0.00	-3.42	0.01	
518181	13.5	6.3		-3.16	0.01	-5.07	0.01	
518180	13.25	6.8		-2.74	0.01	-4.82	0.03	
518179	13	9.3		-3.38	0.00	-4.77	0.01	
518178	12.75	6.3		-2.21	0.01	-6.06	0.03	
518177	12.5	5.8						
518176	12.25	5.8						
518175	12	6.3	0.3	-3.46	0.00	-6.20	0.01	-24.59
518174	11.75	5.3						
518173	11.5	17.1		-8.41	0.00	-6.24	0.00	
518172	11.25	13.7		-10.63	0.01	-4.40	0.02	
518171	11	22.6		-7.17	0.00	-6.67	0.01	
518170	10.75	13.2		-8.95	0.00	-7.30	0.01	
518169	10.5	6.3		-1.40	0.01	-5.45	0.02	
518168	10.25	7.4		-2.01	0.00	-5.35	0.01	-25.12
518167	10	16.3	0.1	-11.12	0.00	-4.20	0.01	
518166	9.75	7.4		-3.76	0.01	-4.35	0.01	
518165	9.5	10.7		-7.75	0.01	-3.20	0.01	
518164	9.25	8.4		-3.89	0.00	-4.47	0.01	
518163	9	10.0		-3.68	0.00	-4.84	0.01	
518162	8.75	6.3		-1.70	0.00	-5.91	0.02	
518161	8.5	5.3						
518160	8.25	5.8						
518159	8	7.4	0.4	-2.49	0.00	-6.85	0.02	-25.25
518158	7.75	8.4		-2.47	0.00	-6.82	0.02	
518157	7.5	4.7						
518156	7.25	0.5						
518155	7	0.0						
518154	6.75	10.0		-1.67	0.00	-5.05	0.01	
518153	6.5	18.4		-3.85	0.00	-5.35	0.02	
518152	6.25	13.7		-2.09	0.01	-4.74	0.01	
518151	6	32.0	0.3	-6.12	0.00	-6.62	0.01	-25.05
518150	5.75	17.9		-5.35	0.00	-6.02	0.01	
518149	5.5	18.4		-5.24	0.00	-5.83	0.01	
518148	5.25	5.8						
518147	5	5.3						
518146	4.75	5.8						
518145	4.5	2.6						
518144	4.25	6.3		-3.79	0.01	-4.83	0.01	
518143	4.1	7.4	0.4	-5.52	0.00	-3.75	0.02	-25.63
518142	3.9	0.0	1.8					-27.47
518141	3	0.0						
518140	2	0.0	3.9					-27.66
518139	1	0.0						
518138	0	0.0	4.2					
n		140	25	53		53		49

Rødryggen Member (38–42 m, 8 samples): The initial interval shows $\delta^{13}C_{org}$ values around -25‰ followed by a peak towards -22.5‰.

Total organic carbon (TOC)

TOC contents are shown in Fig. 2. The black mudstones of the Rødryggen section show a TOC content averaging 3.4% (2.1–4.0%, 5 samples), the Ryazanian–Valanginian mudstones of the Albrechts Bugt Member averaging 0.4% (0–1.9%, 20 samples), the Hauterivian Rødryggen Member averaging 0.1% (0–2.2%, 6 samples) and the Barremian black mudstones averaging 1.1% (0.6–2.8%, 32 samples). The samples from the Perisphinctes Ravine section yield slightly higher TOC contents than those from the Rødryggen section. The underlying black mudstones have a TOC content averaging 3.3% (1.8–4.2%, 3 samples), the mudstones of the Albrechts Bugt and Rødryggen Members average 0.6% (0–1.4%, 17 samples) and 0.5% (0.3–1.2%, 5 samples), respectively.

Major and trace elements

All major and trace element data are documented in the Supplementary data files 1 and 2 available at the web site http://2dgf.dk/publikationer/bulletin/191bull61.html.

Triangular diagrams for both sections, showing the three major chemical components Al_2O_3 (clay minerals), CaO ($CaCO_3$) and SiO_2 (quartz), are illustrated in Fig. 3. In order to centre the data in the graph, arbitrary multipliers (Al_2O_3×5 and CaO×2) were used. Additionally, the composition of average shale following Wedepohl (1971, 1991) is given for comparison. Sediments are composed of a mixture of average shale components with varying amounts of calcium carbonate. A few samples from the Albrechts Bugt Member have higher calcium carbonate or quartz contents compared to the majority of sediments. The Barremian mudstones have in contrast a higher proportion of clay minerals. Relatively high average correlation coefficients of the sections have been observed between SiO_2, Al_2O_3, K_2O, TiO_2 and with trace elements Zr and Rb (except Ba), representing the detrital origin of these elements (Table 3).

Concentrations of all analyzed elements were normalized with respect to Al (element/Al ratios) to compensate for calcium dilution. Major element ratios are expressed as weight ratios, trace element ratios are expressed as weight ratios multiplied by 10^4. This normalization enables one to observe also minor variations in the chemical composition, which otherwise would be masked by changes in the calcium carbonate content. Sediments of the Bernbjerg Formation and Albrechts Bugt Member yield relatively stable Al (Al_2O_3) concentrations similar to average shale (according to Wedepohl 1971, 1991; Table 4). Al concentrations of the Rødryggen Member show a slight decrease in the samples of the Rødryggen section; no major changes have been observed for the Perisphinctes Ravine section. The Barremian black mudstones have the highest Al concentrations.

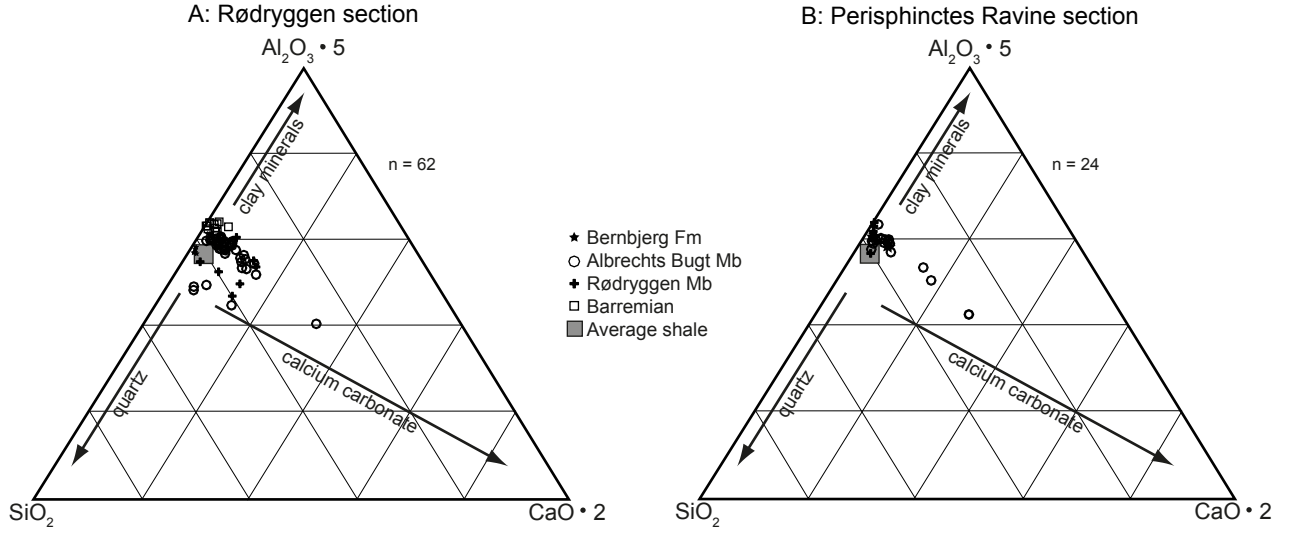

Fig. 3. Ternary diagrams of Al_2O_3×5 – CaO×2 – SiO_2 for the studied sections illustrating the composition of the sediments of the Bernbjerg Formation, Albrechts Bugt and Rødryggen Members and Barremian, in comparison to average shale (Wedepohl 1971, 1991).

Table 3. Correlation coefficients for selected major and trace elements for the Rødryggen and Perisphinctes Ravine sections

Rødryggen section						**Perisphinctes Ravine section**					
	r		r		r		r		r		r
	n = 62		n = 62 (TOC n = 32)		n = 62		n = 24		n = 24		n = 24
SiO_2 - TiO_2	0.440	Al_2O_3 - Co	0.458	U - V	0.605	SiO_2 - TiO_2	0.930	Al_2O_3 - Co	0.034	U - V	0.222
SiO_2 -Al_2O_3	0.396	Al_2O_3 - Cr	0.421	U - Zn	0.284	SiO_2 -Al_2O_3	0.906	Al_2O_3 - Cr	0.035	U - Zn	0.280
SiO_2 - K_2O	0.535	Al_2O_3 - Cu	0.036	U - Cr	0.333	SiO_2 - K_2O	0.911	Al_2O_3 - Cu	0.452	U - Cr	0.222
SiO_2 - Ba	0.295	Al_2O_3 - Mo	-0.009	U - Cu	0.099	SiO_2 - Ba	0.238	Al_2O_3 - Mo	0.275	U - Cu	0.054
SiO_2 - Rb	0.509	Al_2O_3 - Ni	0.469	V - Zn	0.498	SiO_2 - Rb	0.900	Al_2O_3 - Ni	0.059	V - Zn	-0.166
SiO_2 - Zr	0.551	Al_2O_3 - U	0.257	V - Cr	0.529	SiO_2 - Zr	0.685	Al_2O_3 - U	0.239	V - Cr	0.407
TiO_2 - K_2O	0.951	Al_2O_3 - V	0.116	V - Cu	0.011	TiO_2 - K_2O	0.928	Al_2O_3 - V	0.088	V - Cu	-0.419
TiO_2 - Al_2O_3	0.917	Al_2O_3 - Zn	0.035	Zn - Cr	0.425	TiO_2 - Al_2O_3	0.967	Al_2O_3 - Zn	0.385	Zn - Cr	-0.040
TiO_2 - Ba	0.071	TOC - Co/Al	-0.586	Zn - Cu	0.387	TiO_2 - Ba	0.431	TOC - Co/Al	-0.128	Zn - Cu	0.736
TiO_2 - Rb	0.881	TOC - Cr/Al	0.367	Cr - Cu	0.178	TiO_2 - Rb	0.937	TOC - Cr/Al	0.393	Cr - Cu	-0.061
TiO_2 - Zr	-0.023	TOC - Cu/Al	-0.303			TiO_2 - Zr	0.730	TOC - Cu/Al	-0.548		
Al_2O_3 - K_2O	0.927	TOC - Mo/Al	0.646			Al_2O_3 - K_2O	0.904	TOC - Mo/Al	0.729		
Al_2O_3 - Ba	0.053	TOC - Ni/Al	-0.608			Al_2O_3 - Ba	0.367	TOC - Ni/Al	-0.053		
Al_2O_3 - Rb	0.932	TOC - U/Al	0.559			Al_2O_3 - Rb	0.972	TOC - U/Al	0.210		
Al_2O_3 - Zr	-0.209	TOC - V/Al	0.620			Al_2O_3 - Zr	0.617	TOC - V/Al	0.914		
K_2O - Ba	0.068	TOC - Zn/Al	-0.038			K_2O - Ba	0.169	TOC - Zn/Al	-0.249		
K_2O - Rb	0.960	Mo - U	0.560			K_2O - Rb	0.982	Mo - U	0.285		
K_2O - Zr	0.004	Mo - V	0.721			K_2O - Zr	0.773	Mo - V	0.926		
Ba - Rb	0.118	Mo - Zn	0.012			Ba - Rb	0.104	Mo - Zn	-0.208		
Ba - Zr	0.206	Mo - Cr	0.265			Ba - Zr	0.277	Mo - Cr	0.266		
Rb - Zr	-0.069	Mo - Cu	-0.153			Rb - Zr	0.777	Mo - Cu	0.429		

Table 4. Average major and trace element/Al ratios for the different lithological units of the Rødryggen and Perisphinctes Ravine sections

	Rødryggen section				**Perisphinctes Ravine section**			
	Bernbjerg Fm.	Albrechts Bugt Mb.	Rødryggen Mb.	Barremian	Bernbjerg Fm.	Albrechts Bugt Mb.	Rødryggen Mb.	average shale Wedepohl 1971, 1991
	n = 6	n = 32	n = 8	n = 16	n = 3	n = 17	n = 4	
CaCO3 [%]	0.2	10.4 (n = 94)	12.7 (n = 25)	2.1 (n = 32)	0	6.5 (n = 120)	0.6 (n = 15)	3.9
TOC [%]	3.4 (n = 5)	0.4 (n = 20)	0.1 (n = 6)	1.1 (n = 32)	3.3	0.6	0.5 (n = 5)	0.2
Al [%]	8.83	8.86	8.16	10.28	9.13	9.07	10.01	8.89
Si/Al	2.92	2.83	2.95	2.53	2.73	2.72	2.64	3.05
Ti/Al	0.049	0.051	0.051	0.057	0.048	0.051	0.051	0.053
Fe/Al	0.43	0.46	0.65	0.42	0.37	0.53	0.65	0.54
K/Al	0.24	0.24	0.25	0.26	0.25	0.26	0.28	0.32
Ba/Al	69	69	70	56	60	73	63	65
Co/Al	0.1	1.7	1.5	2.0	0.6	1.8	1.5	2.1
Cr/Al	13.8	9.2	11.4	11.2	12.7	9.9	11.4	10.1
Cu/Al	4	5	2	5	2	4	4	10
Mo/Al	6.19	–	–	–	2.48	–	–	0.15
Ni/Al	1.6	4.5	6.2	6.1	3.6	5.8	6.2	7.6
Pb/Al	3.1	2.7	3.3	2.5	3.0	2.8	2.3	2.5
Rb/Al	12.57	12.44	13.07	12.30	12.60	13.50	14.24	15.75
Sr/Al	16.90	27.92	35.00	11.57	15.68	25.58	12.95	33.75
U/Al	0.893	0.533	0.525	0.498	0.695	0.524	0.448	0.416
V/Al	58	15	19	23	39	16	18	15
Zn/Al	11	9	9	11	9	9	9	11
Zr/Al	20	28	35	25	20	24	25	18

Major element ratios are given as weight ratios; trace element ratios are expressed as weight ratios multiplied by10^4

Major element/Al ratios (Si, Ti, K, Zr), being important for the characterization of the detrital matter content, are given in Figs. 4, 5. Si/Al and Zr/Al are relatively constant throughout the studied interval, but both show distinctive peaks in the uppermost part of the Albrechts Bugt Member of the Rødryggen section. Ti/Al and K/Al underlie a relatively stable developing in the Bernbjerg Formation – Rødryggen Member but they show higher values in the Barremian. Fe concentrations are on average higher in the Rødryggen Member in contrast to the remaining sediments (Table 4).

In the Rødryggen section, Sr/Al ratios show a strong correlation with the calcium carbonate content; in the Perisphinctes Ravine section this is less pronounced. Ba/Al ratios are similar to average shale throughout the studied intervals, peaking in the lower part of the Albrechts Bugt Member and have lower values in the Barremian.

Redox-sensitive trace elements (Cr, Mo, U, V, Zn) hold relatively high element/Al ratios in the TOC rich Bernbjerg Formation (Figs. 6, 7). Cu/Al and Cr/Al ratios show also marked peaks in the TOC poor Albrechts Bugt and Rødryggen Members. Co, Cu and Ni have varying element/Al ratios, which are below the values of average shale (Table 4). A strong correlation between Co and Ni has been observed in both sections ($r = 0.767$ and $r = 0.974$). The Bernbjerg Formation constitutes a depletion of Co and Ni. Correlation factors between the redox-sensitive elements mutually, as well as between redox-sensitive elements and TOC (Table 3) are relatively high especially for Mo, U and V; they show, however, a relatively low correlation with Al_2O_3.

Discussion

Carbon isotopes

The carbon isotope record of the Cretaceous is marked by several excursions related to perturbations of the carbon cycle (e.g. Weissert 1989; Weissert & Chanell 1989; Menegatti *et al*. 1998; Weissert & Erba 2004; Jenkyns 2010). A prominent feature of the earliest Cretaceous is the mid-Valanginian $\delta^{13}C$-excursion (Lini *et al*. 1992; Channell *et al*. 1993; Weissert & Erba 2004), which is characterized by an excursion from 1 to 3‰. The $\delta^{13}C$-isotope event is documented in the marine carbonate reservoirs, fossil shell material (e.g. belemnite guards) terrestrial (i.e. land plants) and marine organic matter (e.g. Gröcke *et al*. 1999, 2003, 2005; Ferreri *et al*. 1997; Aguirre-Urreta *et al*. 2008; Nunn *et al*. 2010), suggesting this event to be global.

The $\delta^{13}C_{carb}$ values observed in this study (Fig. 2) are on average much lighter than contemporaneous values presented for the Tethyan bulk-rock carbonate (1–3‰) (Weissert & Erba 2004) and belemnite guards (-2 to 1‰) (McArthur *et al*. 2007). Swientek (2003) studied Kimmeridgian–Barremian sediments from Norway and the Barents Sea showing similar $\delta^{13}C_{carb}$ values (-15.5 to 0.3‰) to those of Greenland. The ^{13}C depletion may be explained by early diagenesis accompanied by microbial decomposition of organic matter. Bacterial sulfate reduction and methanogenesis coupled with authigenic carbonate precipitation may have altered the isotopic composition of the sediments (e.g. Berner 1981; Lein 2004; Decampo 2010). Microbial processes produce additional bicarbonate (HCO_3^-), shifting the $\delta^{13}C_{carb}$ composition towards values similar to those of $\delta^{13}C_{org}$ (-28 to -20‰). If methanogenesis would have affected the isotopic composition, $\delta^{13}C_{carb}$ values were expected to be much lighter than those observed. Well-preserved calcareous nannofossils constitute a significant carbonate source in samples with low carbonate contents (Pauly *et al*. 2012b). Samples having relatively high carbonate contents are characterized by moderate to poorly preserved nannofossil assemblages, micrite-rich or even barren samples, which support the consideration of authigenic carbonate precipitation.

The $\delta^{13}C_{org}$ values of the investigated sediments (average -25‰; Fig. 2) are similar to $\delta^{13}C_{org}$ values recorded for marine sediments from offshore Morocco, France and Poland (Wortmann & Weissert 2000; Kujau *et al*. 2013), allowing us to exclude major diagenetic alteration. The $\delta^{13}C_{org}$ values of the TOC-rich Bernbjerg Formation are slightly lighter (2–3‰) than those of the remaining sediments. This ^{13}C depletion may indicate bacterial sulfate reduction, which is very likely in the oxygen-depleted depositional environment of the Bernbjerg Formation (Surlyk 1977; Strogen et al 2005). The $\delta^{13}C_{org}$ values of the Albrechts Bugt Member, Rødryggen Member and Barremian are relatively stable (around -25‰). Strong deviations may indicate a poor preservation of organic matter, changing ratios of marine and terrestrial organic matter, or early diagenesis (bacterial sulfate reduction and authigenic carbonate formation). The well-defined $\delta^{13}C$ excursion, however, is not recorded in the Valanginian sediments from North-East Greenland, either due to the high condensation of the strata and the related sample density, or a hiatus in the sedimentary record.

Major and trace elements

The studied sediments show a significant input of terrigenous material (quartz, clay minerals) similar to average shale and with varying biogenic calcium

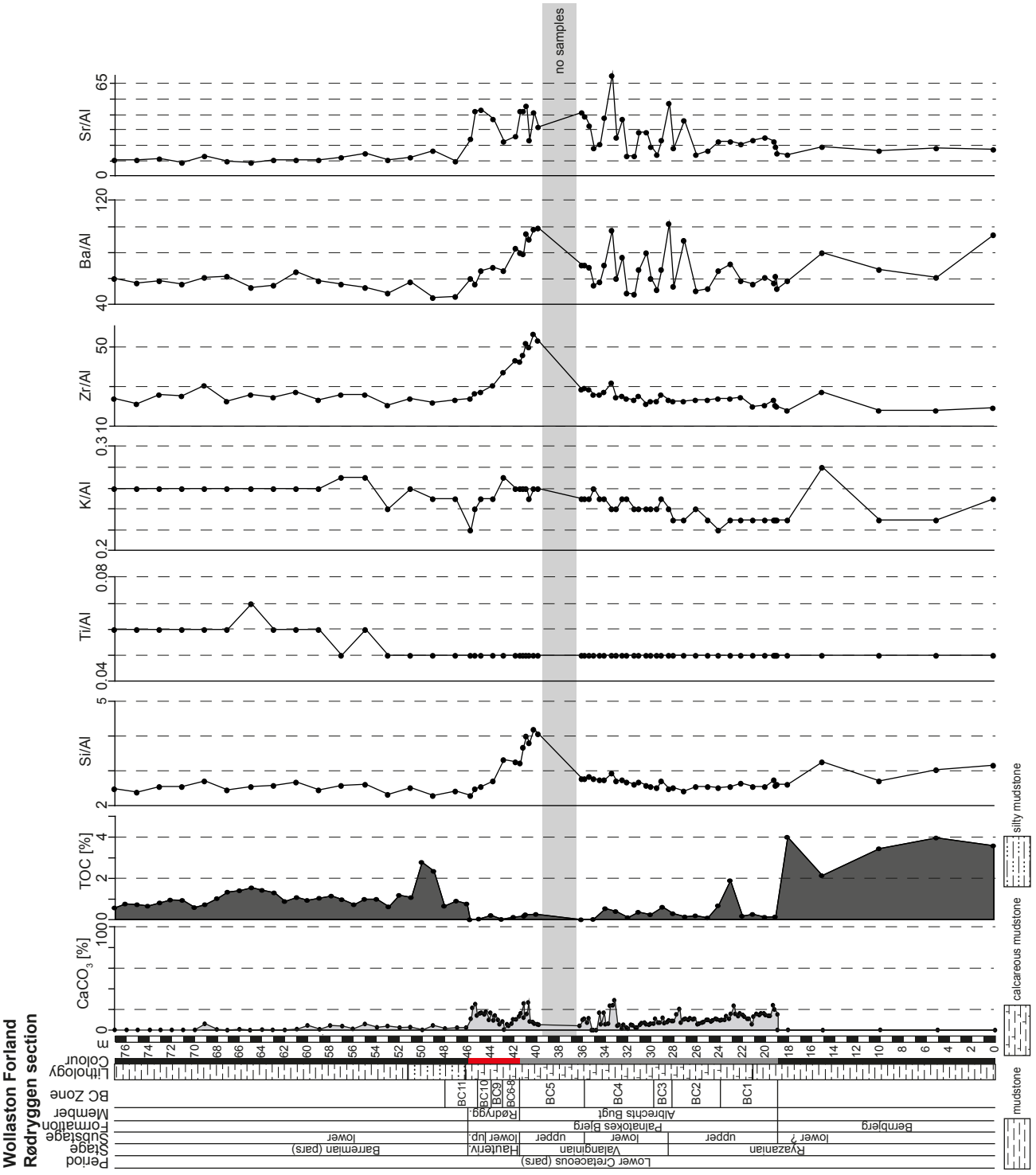

Fig. 4. Lithological log of the Rødryggen section showing the Boreal calcareous nannofossil (BC) zones and $CaCO_3$ (from Pauly *et al*. 2012b) and TOC contents, Si/Al, Ti/Al, K/Al, Zr/Al, Ba/Al and Sr/Al ratios. Major element ratios are given as weight ratios; trace element ratios are expressed as weight ratios multiplied by 10^4.

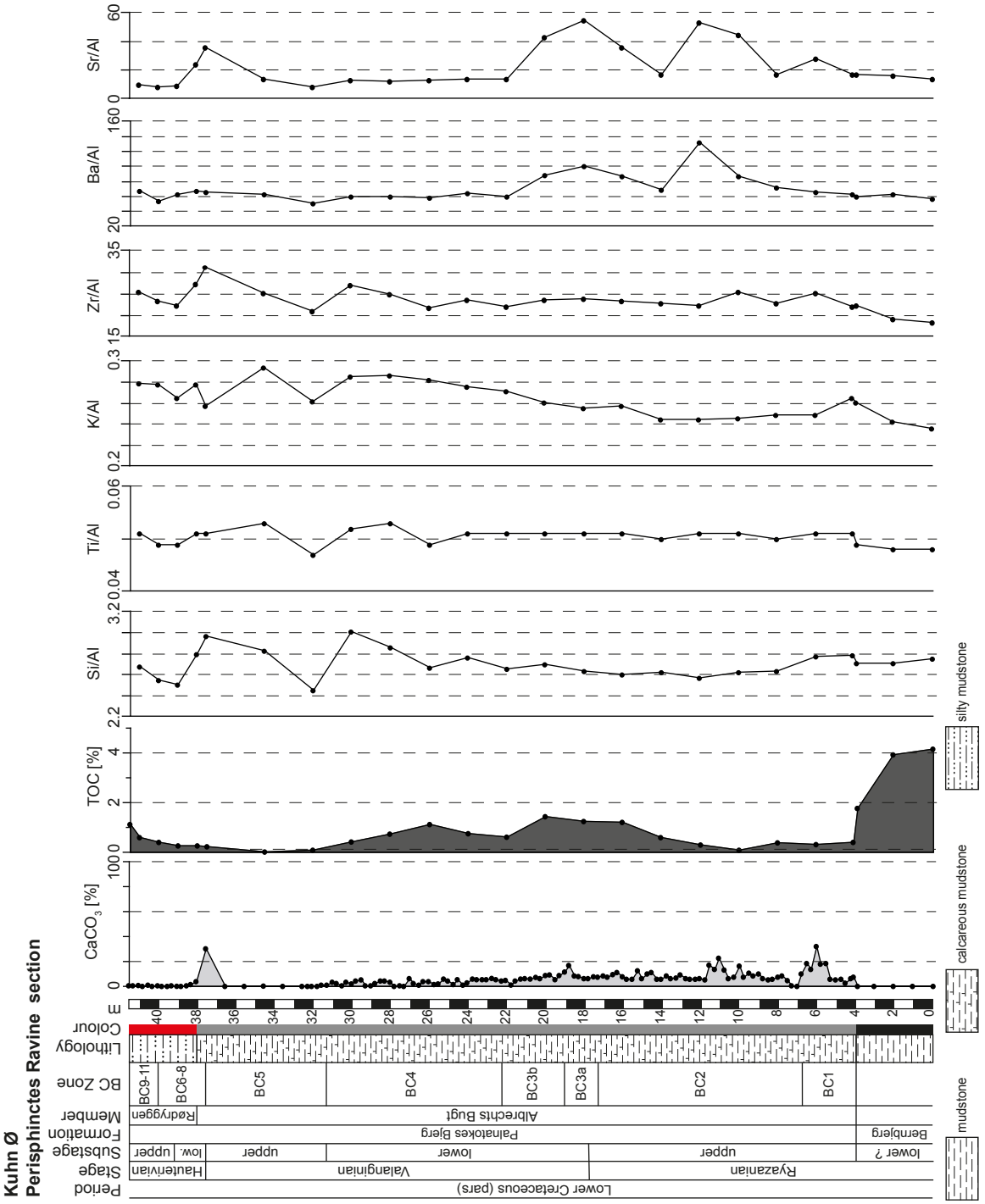

Fig. 5. Lithological log of the Perisphinctes Ravine section showing the Boreal calcareous nannofossil (BC) zones and $CaCO_3$ (from Pauly *et al*. 2012b) and TOC contents, Si/Al, Ti/Al, K/Al, Zr/Al, Ba/Al and Sr/Al ratios. Major element ratios are given as weight ratios; trace element ratios are expressed as weight ratios multiplied by 10^4.

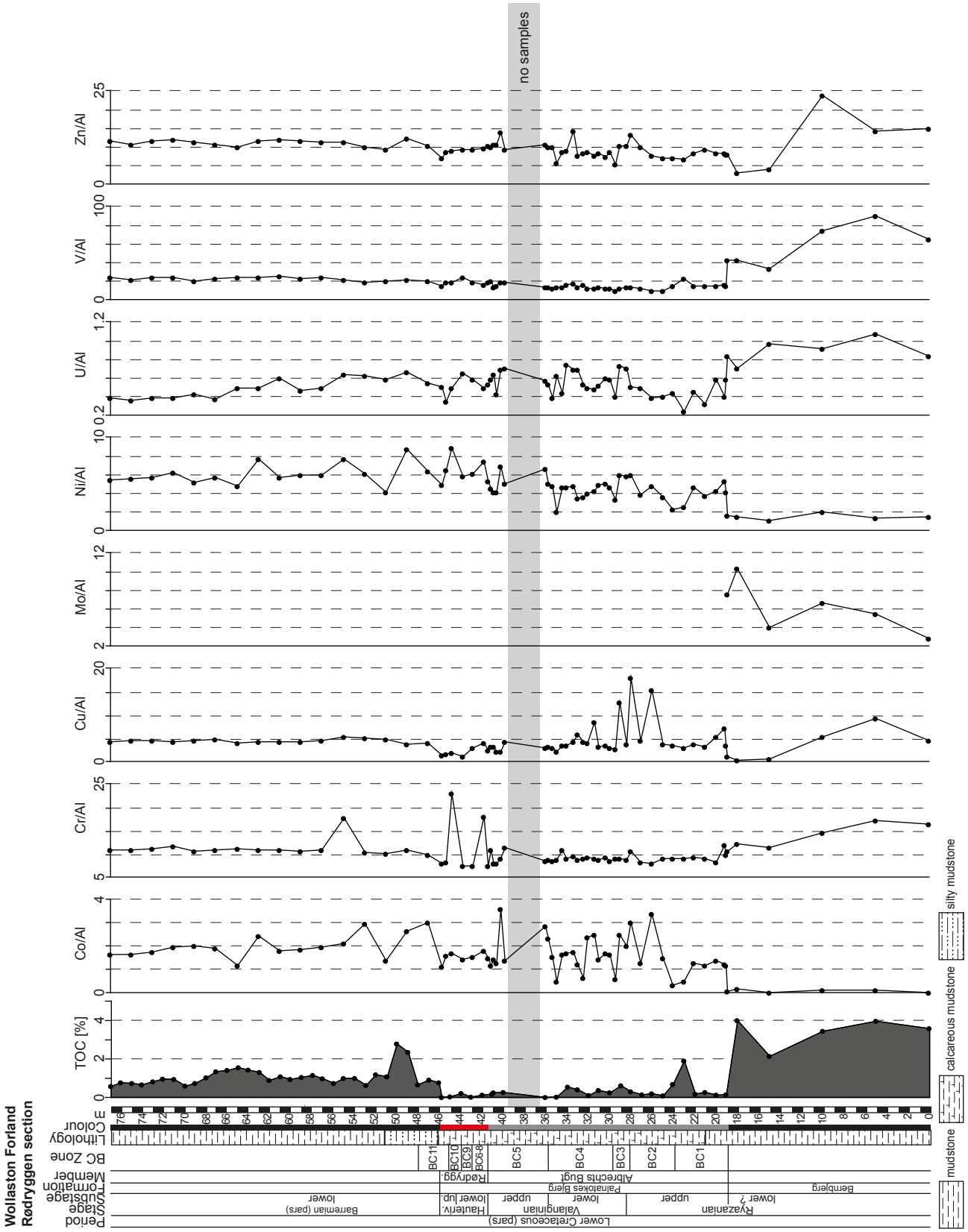

Fig. 6. Lithological log of the Rødryggen section (BC zones from Pauly *et al*. 2012b) showing the TOC contents, Co/Al, Cr/Al, Cu/Al, Mo/Al, Ni/Al, U/Al, V/Al and Zn/Al ratios. Trace element/Al ratios are given as weight ratios multiplied by 10^4.

carbonate concentrations. Although the lithology is relatively uniform throughout the sections, minor variations in the composition of the detrital matter have been observed. These are manifested in changing Si/Al (quartz, clay minerals), K/Al (clay minerals) and Zr/Al (heavy minerals) ratios. The Barremian sediments show increased Ti/Al ratios (heavy minerals) and a higher clay mineral content, which correlate well with the observed increase of the K/Al ratios (Fig. 4, 5).

Major mechanisms controlling the concentration of the trace elements are the rate of terrigenous input, redox conditions during deposition, and the coupling to biogenic cycles in the water column. Strontium shows a strong correlation with Ca because it is fixed

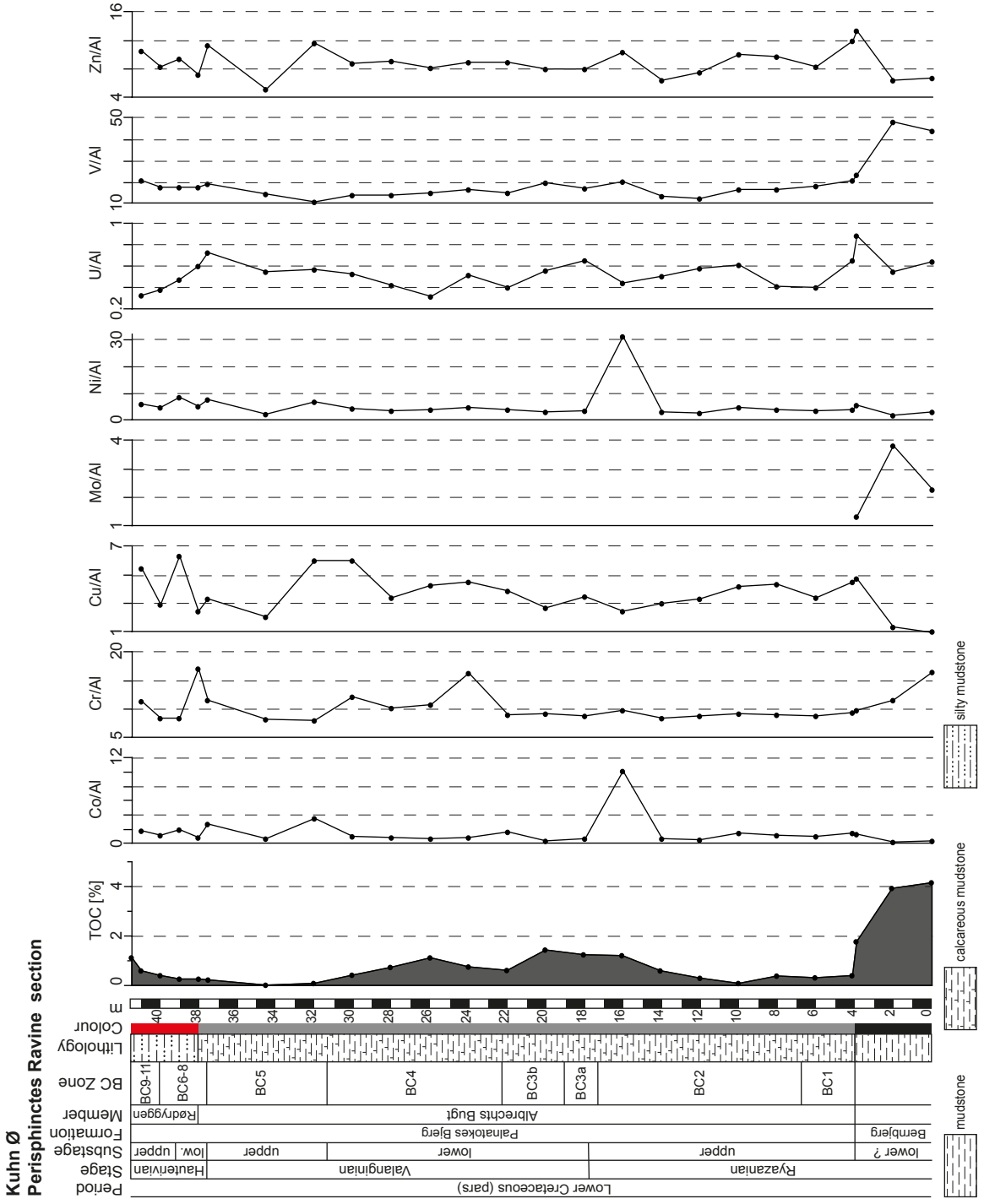

Fig. 7. Lithological log of the Perisphinctes Ravine section (BC zones from Pauly *et al.* 2012b) showing the TOC contents, Co/Al, Cr/Al, Cu/Al, Mo/Al, Ni/Al, U/Al, V/Al and Zn/Al ratios. Trace element/Al ratios are given as weight ratios multiplied by 10^4.

in the carbonate lattice where it can substitute Ca. Barium is considered to be indicative for high palaeoproductivity (e.g. McManus *et al*. 1998; Gingele *et al*. 1999; Bains *et al*. 2000; Prakash Babu *et al*. 2002). The observed Ba/Al ratios suggest an average productivity for the Ryazanian–Hauterivian with phases of increased productivity during the early Valanginian and a reduced productivity in the Barremian, which is in accordance with the total nannofossil abundance (Pauly *et al*. 2012b).

Redox-sensitive trace elements (Cr, Mo, U, V, Zn) in organic-rich sediments are commonly used as indicators for redox conditions during deposition (e.g. Brumsack & Gieskes 1983; Algeo & Maynard 2004; Tribovillard *et al*. 2004, 2005, 2006; Brumsack 2006). Under anoxic conditions, Mo, V and U show a relatively low enrichment in the sediment but a relatively high correlation with TOC, because the uptake of trace elements is mainly limited by the availability of organic matter (Algeo & Maynard 2004, Tribovillard *et al*. 2006). Under euxinic conditions (free H_2S), insoluble metal sulphides or oxyhydroxides can precipitate directly from the water column or at the sediment–water interface, which results in strong enrichments of Mo, V and U and weak correlations with TOC (Algeo & Maynard, 2004; Tribovillard *et al*. 2004, 2006). The sediments of the Bernbjerg Formation show a good correlation of trace elements (Mo,V, U) with TOC (Figs 6,7; Table 3), implying coupling to organic matter. Although a concurrent enrichment in U, V and Mo could be recognized, concentrations of redox-sensitive trace elements are mostly lower (e.g. Mo: average 50 ppm, max. 100 ppm) in comparison to modern euxinic environments (Mo: 70–160 ppm) observed by e.g. Lyons *et al*. (2009). The enrichment of the redox-sensitive elements (Mo, U, V) together with relatively high TOC concentrations in the Bernbjerg Formation thus indicates predominantly anoxic bottom water conditions with occasional free H_2S.

Observed peaks of Cu and Cr in the well-oxygenated Albrechts Bugt and Rødryggen Members are suggestive of a detrital origin, these elements residing in oxides or hydroxides. Cobalt has a chemical behaviour like Mn, forming insoluble sulphide (CoS) that can be taken up in solid solution by authigenic Fe-sulphides (Huerta-Diaz & Morse 1992; Algeo & Maynard 2004). Cobalt concentrations may be limited in authigenic sulphides as Co uptake is kinetically slow (Morse & Luther 1999). It is also uncertain to which extent Co is influenced by the Fe–Mn redox cycling (Algeo & Maynard 2004). The depletion of Ni in the Bernbjerg Formation, which on the other hand is enriched in redox-sensitive trace elements, may imply lowered Ni concentrations in the seawater or post-sedimentary diagenesis. The depletion of Co and Cu in the seawater in the Greenland–Norwegian Seaway is probably related to decreased sediment transport that may explain the low concentrations of these elements in comparison to average shale. Following Tribovillard *et al.* (2006) Co is under a strong detrital influence that rather limits the use as a reliable redox proxy.

Depositional environment

The Bernbjerg Formation (Kimmeridgian/early Ryazanian), composed of black, rhythmically laminated, non-bioturbated, silt-rich mudstones, has been viewed as a low-energy, euxinic shelf facies (Surlyk 1977; Surlyk & Clemmensen 1975a; Surlyk & Clemmensen 1983). Relatively high contents of organic matter and the enrichment of redox-sensitive trace elements support the interpretation of anoxic bottom water conditions with occasional free H_2S during the deposition of this formation (Fig. 8), similar to the Volgian–Ryazanian sedimentary units of mid and north Norway (Mutterlose *et al*. 2003).

The Albrechts Bugt Member (late Ryazanian to Valanginian), consisting of light grey laminated calcareous mudstones, is characterized by low TOC contents, rich benthic fauna, common trace fossils (*Zoophycos*, *Thalassinoides*), ammonites, belemnites, brachiopods and bivalves (Surlyk & Clemmensen 1975a; Surlyk 1978; Alsen 2006; Alsen & Mutterlose 2009). Calcareous nannofossils and unidentifiable micrite constitute the major carbonate source of the Albrechts Bugt Member (Pauly *et al*. 2012b), forming thereby the first calcareous sediments in North-East Greenland since the late Permian (Maync 1949; Alsen 2006). The sedimentological, palaeontological and geochemical analyses indicate a low-energy open marine shelf environment below the storm wave base, hemipelagic sedimentation of fine-grained terrigenous material, biogenic carbonate production, and well-oxygenated sea-floor conditions. Surface water temperatures were cool to cold with changing surface water fertility (mesotrophic–oligotrophic) as suggested by fluctuation of the calcareous nannofossil assemblages (Pauly *et al*. 2012b) and varying Ba concentrations.

The Rødryggen Member (Hauterivian) is composed of red, calcareous mudstones with almost no sedimentary structures (Surlyk & Clemmensen 1975a). Similar to the underlying Albrechts Bugt Member, the calcium carbonate is derived mainly from calcareous nannofossils and unidentifiable micrite (Pauly *et al*. 2012b). The colour is based on a high content of oxidized iron minerals (haematite and goethite), derived from weathering in the hinterland (Alsen 2006). This view is promoted by the observed increase of Fe/Al ratios and increased surface water fertility during warm climatic conditions (Pauly *et al*. 2012b).

The Barremian black laminated mudstones, devoid of benthic fossils and trace fossils (Surlyk 1978) and with slightly increased TOC values, mark a major palaeoceanographic change from well oxygenated to likely dysoxic bottom water conditions. This, however, is not supported by the redox-sensitive trace element data (V/Al, U/Al, Cr/Al and Cu/Al ratios) that show comparable values to the Albrechts Bugt and the Rødryggen Member. Biogenic carbonate formation by calcareous nannoplankton declined in the Barremian although it is difficult to distinguish between primary signals (primary productivity) and preservation effects.

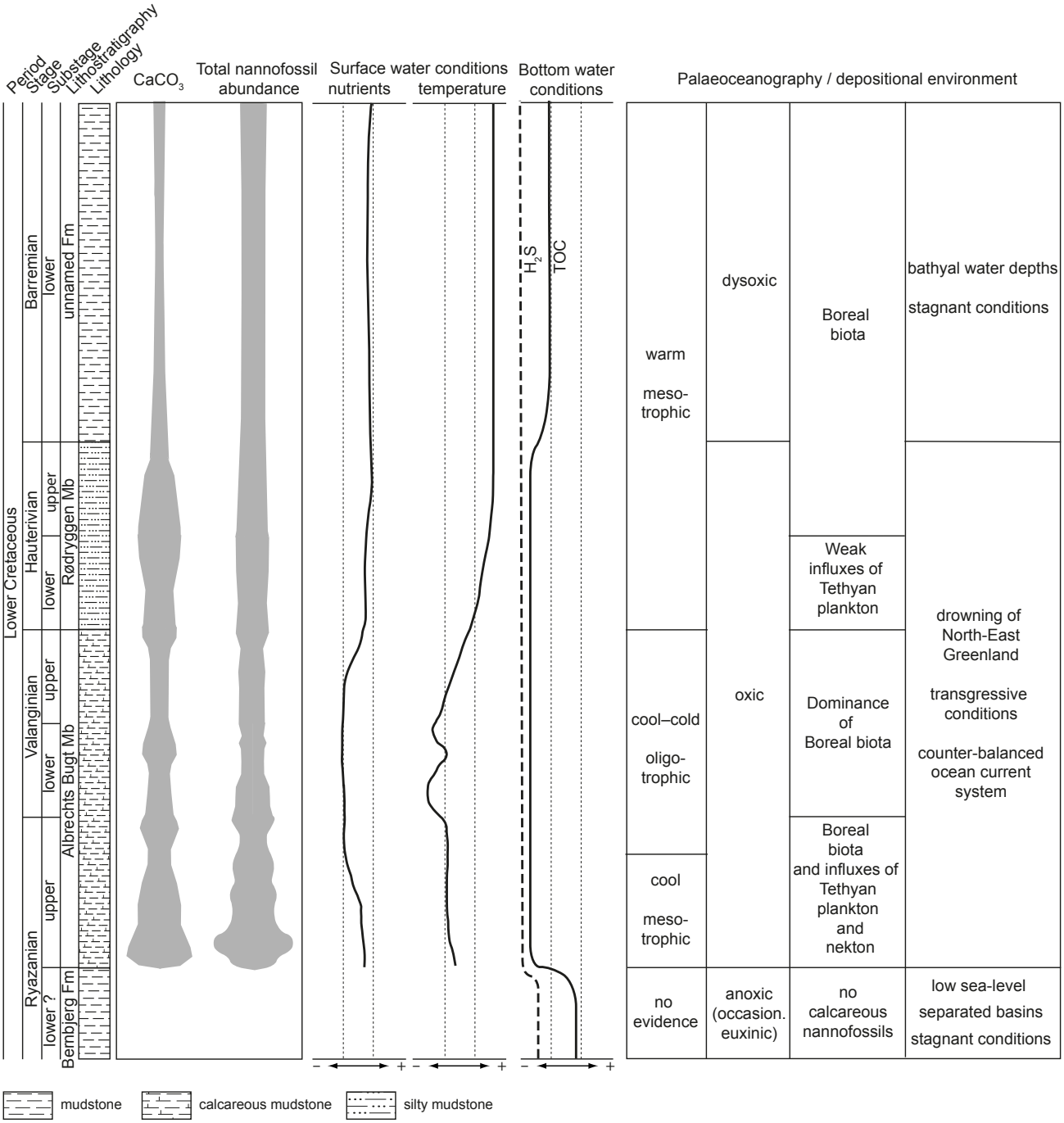

Fig. 8. Synthesis of the most important findings and their implications for palaeoceanography and depositional environments. $CaCO_3$ content and total nannofossil abundance taken from Pauly *et al.* (2012b); palaeoceanography and depositional environment from Alsen 2006 and references therein, and Pauly *et al.* (2012b).

Conclusions

The $\delta^{13}C_{org}$ curve presents the first record of this kind for the Lower Cretaceous (upper Ryazanian – Barremian) of North-East Greenland. The well-defined mid-Valanginian carbon isotope excursion has not been recorded, either due to condensation of the lower Cretaceous sediment units or a hiatus in the sedimentary record. The $\delta^{13}C_{carb}$ values exhibit strong ^{13}C depletion, indicating early diagenesis accompanied by microbial decomposition of organic matter.

The Lower Cretaceous sediments are characterized by a mixture of terrigenous detrital matter (quartz, clay minerals, heavy minerals) similar to average shale and with varying $CaCO_3$ concentrations. The Barremian black mudstones have lower calcium carbonate and higher clay mineral contents than the underlying sediments.

The deposition of the Bernbjerg Formation took place under prevailing anoxic bottom water conditions related to a low sea-level, separated basins and restricted conditions (Fig. 8). The depositional environment of the Albrechts Bugt and Rødryggen Members is characterized by well-oxygenated sea-floor conditions, hemipelagic sedimentation of fine-grained terrigenous detrital matter and biogenic carbonate settling. This relatively short period of carbonate sedimentation was followed by a decrease of carbonate accumulation and a return of likely dysoxic bottom water conditions. Bathyal water depths and a sluggish ocean circulation during the Barremian caused stagnant conditions and thereby the burial of organic matter.

During most of the Jurassic and Early Cretaceous stagnant bottom water masses resulted in the deposition of black mudstones in the Greenland–Norwegian Seaway (Mutterlose *et al*. 2003). A change to well oxygenated sea-floor conditions took place during a relatively short period with deposition of calcareous sediments. This palaeoceanographic change is also recorded in contemporaneous sediments in the north-eastern part of the Greenland–Norwegian Seaway, the Klippfisk and Lange Formations (offshore Norway) (Århus *et al*. 1990; Århus, 1991; Smelror *et al*. 1998; Mutterlose *et al*. 2003) and the Leira and Skjermyrbekken Members at Andøy (North Norway) (Dalland 1975).

Acknowledgements

GEUS (Geological Survey of Denmark and Greenland) and its members are thanked for field work management, assistance, and collaboration. We are grateful to N. Andersen (CAU Kiel) for $\delta^{13}C_{carb}$ and M. Joachimski (GeoZentrum Nordbayern) for $\delta^{13}C_{org}$ analyses. T. Goral (Ruhr-University Bochum) is thanked for carbon measurements and H. Brumsack (University of Oldenburg) for major and trace element analyses. We also thank L. Clemmensen and M. Lenniger for their helpful comments on the manuscript. Financial support by the German Research Foundation (DFG, MU 667/38-1) is gratefully acknowledged.

References

Aguirre-Urreta, M.B., Price, G.D., Ruffell, A.H., Lazo, D.G., Kalin, R.M., Ogle, N. & Rawson, P.F. 2008: Southern Hemisphere Early Cretaceous (Valanginian–Early Barremian) carbon and oxygen isotope curves from the Neuquén Basin, Argentina. Cretaceous Research 29 (1), 87–99.

Algeo, T.J. & Maynard, J.B. 2004: Trace-element behaviour and redox facies in core shales of Upper Pennsylvanian Kansas-type cyclothems. Chemical Geology 206, 289–318.

Alsen, P. 2006: The Early Cretaceous (Late Ryazanian–Early Hauterivian) ammonite fauna of North-East Greenland: taxonomy, biostratigraphy, and biogeography. Fossils and Strata 53, 229 pp.

Alsen, P. & Mutterlose, J. 2009: The Early Cretaceous of North-East Greenland: A crossroads of belemnite migration. Palaeogeography, Palaeoclimatology, Palaeoecology 280, 168–182.

Alsen, P. & Rawson, P.F. 2005: The Early Valanginian (Early Cretaceous) ammonite *Delphinites* (*Pseudogarniera*) from North-East Greenland. Bulletin of the Geological Society of Denmark 52, 201–212.

Århus, N. 1991: The transition from deposition of condensed carbonates to dark claystones in the Lower Cretaceous succession of the southwestern Barents Sea. Norsk Geologisk Tidsskrift 71, 259–263.

Århus, N., Kelly, S.R.A., Collins, J.S.H. & Sandy, M.R. 1990: Systematic palaeontology and biostratigraphy of two Early Cretaceous condensed sections from the Barents Sea. Polar Research 8, 165–194.

Bains, S., Norris, R.D., Corfield, R.M. & Faul, K.L. 2000: Termination of global warmth at the Palaeocene/Eocene boundary through productivity feedback. Nature 407, 171–174.

Berner, R.A., 1981: A new geochemical classification of sedimentary environments. Journal of Sedimentary Petrology 51, 359–365.

Brumsack, H.-J. 2006: The trace metal content of recent organic carbon-rich sediments: Implication for Cretaceous black shale formation. Palaeogeography, Palaeoclimatology, Palaeoecology 232 (2-4), 344–361.

Brumsack, H.-J. & Gieskes, J.M. 1983: Interstitial water trace-metal chemistry of laminated sediments from the Gulf of California, Mexico. Marine Chemistry 14, 89–106.

Channell, J.E.T., Erba, E. & Lini, A. 1993: Magnetostratigraphic

calibration of the late Valanginian carbon isotope event in pelagic limestones from northern Italy and Switzerland. Earth and Planetary Science Letters 118, 145–166.

Dalland, A. 1975: The Mesozoic rocks of Andøy, Northern Norway. Norges Geologiske Undersøgelse Bulletin 316, 271–287.

Decampo, D.M. 2010: The Geochemistry of Continental Carbonates. In: Alonso-Zarza, A.M. & Tanner, L.H. (eds), Carbonates in Continental Settings, Geochemistry, Diagenesis and Applications. Developments in Sedimentology 62, 1–59. Amsterdam: Elsevier.

Ferreri, V., Weissert, H., D'Argenio, B. & Buonocunto, F.P. 1997: Carbon isotope stratigraphy: a tool for basin to carbonate platform correlation. Terra Nova 9, 57–61.

Gingele, F.X., Zabel, M., Kasten, S., Bonn, W.J. & Nurnberg, C.C. 1999: Biogenic barium as a proxy for paleoproductivity: Methods and limitations of application. In: Fischer, G. & Wefer, G. (eds), Use of Proxies in Paleoceanography, 345–364. Berlin: Springer-Verlag.

Gröcke, D.R., Hesselbo, S.P. & Jenkyns, H.C. 1999: Carbon isotope composition of Lower Cretaceous fossil wood; ocean–atmosphere chemistry and relation to sea-level change. Geology 27, 155–158.

Gröcke, D.R., Price, G.D., Baraboshkin, E., Mutterlose, J. & Ruffell, A.H. 2003: The Valanginian terrestrial carbon isotope record. Geophysical Research Abstracts 5.

Gröcke, D.R., Price, G.D., Robinson, S.A., Baraboshkin, E.Y., Mutterlose, J. & Ruffell, A.H. 2005: The Upper Valanginian (Early Cretaceous) positive carbon isotope event recorded in terrestrial plants. Earth and Planetary Science Letters 240, 495–509.

Harper, D.A.T., Alsen, P., Owen, E.F. & Sandy, M.R. 2005: Early Cretaceous brachiopods from East Greenland: biofacies and biogeography. Bulletin of the Geological Society of Denmark 52, 213–225.

Huerta-Diaz, M.G. & Morse, J.W. 1992: Pyritization of trace metals in anoxic marine sediments. Geochimica et Cosmochimica Acta 56, 2681–2702.

Jenkyns, H.C. 2010: Geochemistry of oceanic anoxic events. Geochemistry, Geophysics, Geosystems 11 (3), Q03004, doi: 10.1029/2009GC002788.

Kujau, A., Heimhofer, U., Hochuli, P., Pauly, S., Morales, C., Adatte, T., Föllmi, K.B., Ploch, I. & Mutterlose, J. 2013: Reconstructing Valanginian (Early Cretaceous) mid-latitude vegetation and climate dynamics based on spore-pollen assemblages. Review of Palaeobotony and Palynology 197, 50–69.

Lein, A.Y. 2004: Authigenic carbonate formation in the ocean. Lithology and Mineral Resources 39, 1–30.

Lini, A., Weissert, H. & Erba, E. 1992: The Valanginian carbon isotope event: a first episode of greenhouse climate conditions during the Cretaceous. Terra Nova 4, 374–384.

Lyons, T.W., Anbar, A.D., Severmann, S., Scott, C. & Gill, B. 2009: Tracking euxinia in the ancient ocean: a multiproxy perspective and Proterozoic case study. Annual Review of Earth and Planetary Sciences 37, 507–34.

Maync, W. 1949: The Cretaceous beds between Kuhn Island and Cape Franklin (Gauss Peninsula), Northern East Greenland. Meddelelser om Grønland 133 (3), 291 pp.

McArthur, J.M., Janssen, N.M.M., Reboulet, S., Leng, M.J., Thirlwall, M.F. & van de Schootbrugge, B. 2007: Palaeotemperatures, polar ice-volume, and isotope stratigraphy (Mg/Ca, $\delta^{18}O$, $\delta^{13}C$, $^{87}Sr/^{86}Sr$): The Early Cretaceous (Berriasian, Valanginian, Hauterivian). Palaeogeography, Palaeoclimatology, Palaeoecology 248, 391–430.

McManus, J. *et al.* 1998: Geochemistry of barium in marine sediments: Implications for its use as a paleoproxy. Geochimica et Cosmochimica Acta 62, 3453–3473.

Menegatti, A.P., Weissert, H., Brown, R.S., Tyson, R.V., Farrimond, P., Strasser, A. & Caron, M. 1998: High-resolution $\delta^{13}C$-stratigraphy through the early Aptian "Livello Selli" of the Alpine Tethys. Paleoceanography 13, 530–545.

Morse, J.W. & Luther III, G.W. 1999: Chemical influences on trace metal-sulphide interactions in anoxic sediments. Geochimica et Cosmochimica Acta 63, 3373–3378.

Mutterlose, J. *et al* 2003: The Greenland–Norwegian Seaway: A key area for understanding Late Jurassic to Early Cretaceous paleoenvironments. Paleoceanography 18 (1), 1–26.

Nøhr-Hansen, H. 1993: Dinoflagellate cyst stratigraphy of the Barremian to Albian, Lower Cretaceous, North-East Greenland. Bulletin Grønlands Geologiske Undersøgelse 166, 171 pp.

Nunn, E.V., Price, G.D., Gröcke, D.R., Baraboshkin, E.Y., Leng, M.J. & Hart, M.B. 2010: The Valanginian positive carbon isotope event in Arctic Russia: evidence from terrestrial and marine isotope records and implications for global carbon cycling. Cretaceous Research 31 (6), 577–592.

Pauly, S., Mutterlose, J. & Alsen, P. 2012a: Lower Cretaceous (upper Ryazanian–Hauterivian) chronostratigraphy of high latitudes (North-East Greenland). Cretaceous Research 34, 308–326.

Pauly, S., Mutterlose, J. & Alsen, P. 2012b: Early Cretaceous palaeoceanography of the Greenland–Norwegian Seaway evidenced by calcareous nannofossils. Marine Micropaleontology 90–91, 72–85.

Prakash Babu, C., Brumsack, H.-J., Schnetger, B. & Böttcher, M.E. 2002: Barium as a productivity proxy in continental margin sediments: a study from the eastern Arabian Sea. Marine Geology 184, 189–206.

Smelror, M., Mørk, A., Monteil, E., Rutledge, D. & Leereveld, H. 1998: The Klippfisk Formation – a new lithostratigraphic unit of Lower Cretaceous platform carbonates on the Western Barents Shelf. Polar Research 17 (2), 181–202.

Strogen, D.P., Burwood, R. & Whitham, A.G. 2005: Sedimentology and geochemistry of Late Jurassic organic-rich shelfal mudstones from East Greenland: regional and stratigraphic variations in source-rock quality. In: Doré, A.G. & Vining, B.A. (eds): Petroleum Geology: North-West Europe and Global Perspectives. Proceedings of the 6th Petroleum Geology Conference, 903–912. London: The Geological Society.

Surlyk, F. 1977: Stratigraphy, tectonics and palaeogeography of the Jurassic sediments of the areas north of Kong Oscars Fjord, East Greenland. Bulletin Grønlands Geologiske Undersøgelse 123, 56 pp.

Surlyk, F. 1978: Submarine fan sedimentation along fault scarps on tilted fault blocks (Jurassic–Cretaceous boundary, East Greenland). Bulletin Grønlands Geologiske Undersøgelse 128, 108 pp.

Surlyk, F. 1984: Fan-delta to submarine fan conglomerates of the Volgian–Valanginian Wollaston Forland Group, East Greenland. In: Koster, E.H. & Steel, R.J. (eds), Sedimentology of gravels and conglomerates. Canadian Society of Petroleum Geologists, Memoir 10, 359–382.

Surlyk, F. 1990: A Jurassic sea-level curve for East Greenland. Palaeogeography, Palaeoclimatology, Palaeoecology 78, 71–85.

Surlyk, F. 2003: The Jurassic of East Greenland: a sedimentary record of thermal subsidence, onset and culmination of rifting. Geological Survey of Denmark and Greenland Bulletin 1, 659–722.

Surlyk, F. & Clemmensen, L.B. 1975a: A Valanginian turbidite sequence and its palaegeographical setting (Kuhn Ø, East Greenland). Geological Society of Denmark Bulletin 24, 61–73.

Surlyk, F. & Clemmensen, L.B. 1975b: Sedimentology and stratigraphy of the Middle Jurassic–Lower Cretaceous rocks of the Wollaston Forland–Kuhn Ø area, central East Greenland. Rapport Grønlands Geologiske Undersøgelse 75, 110–115.

Surlyk, F. & Clemmensen, L.B. 1983: Rift progradation and eustacy as controlling factors during Jurassic inshore and shelf sedimentation in northern East Greenland. Sedimentary Geology 34, 119–143.

Surlyk, F., Callomon, J.H., Bromley, R.G. & Birkelund, T. 1973: Stratigraphy of the Jurassic–Lower Cretaceous sediments of Jameson Land and Scoresby Land, East Greenland. Bulletin Grønlands Geologiske Undersøgelse 105, 76 pp.

Swientek, O. 2003: The Greenland–Norwegian Seaway: climatic and cyclic evolution of Late Jurassic–Early Cretaceous sediments. Inaugural Dissertation, PhD thesis, University of Cologne, Germany, 148 pp.

Tribovillard, N., Riboulleau, A., Lyons, T. & Baudin, F. 2004: Enhanced trapping of molybdenum by sulfurized marine organic matter of marine origin in Mesozoic limestones and shales. Chemical Geology 213, 385–401.

Tribovillard, N., Ramdani, A. & Trentesaux, A. 2005: Controls on organic accumulation in Late Jurassic shales of northwestern Europe as inferred from trace-metal geochemistry. In: Harris, N. (ed.), The Deposition of Organic-Carbon-Rich Sediments: Models, Mechanisms, and Consequences. SEPM Special Publication 82, 145–164.

Tribovillard, N., Algeo, T.J., Lyons, T. & Riboulleau, A. 2006: Trace metals as paleoredox and paleoproductivity proxies: an update. Chemical Geology 232, 12–32.

Wedepohl, K.H. 1971: Environmental influences on the chemical composition of shales and clays. In: Ahrens, L. H., Press, F., Runcorn, S. K. & Urey, H. C. (eds), Physics and Chemistry of the Earth, 305–333. Oxford: Pergamon.

Wedepohl, K.H. 1991: The composition of the upper earth's crust and the natural cycles of selected metals. Metals in natural raw materials. Natural resources. In: Merian, E. (ed.), Metals and their compounds in the environment, 3–17. Weinheim: VCH-Verlagsgesellschaft.

Weissert, H. 1989: C-isotope stratigraphy, a monitor of paleoenvironmental change: a case study from the early Cretaceous. Surveys in Geophysics 10, 1–61.

Weissert, H. & Channell, J.E.T. 1989: Tethyan carbonate carbon isotope stratigraphy across the Jurassic–Cretaceous boundary: an indicator of decelerated carbon cycling. Paleoceanography 4, 483–494.

Weissert, H. & Erba, E. 2004: Volcanism, CO_2 and palaeoclimate: a Late Jurassic–Early Cretaceous carbon and oxygen isotope record. Journal of the Geological Society, London 161, 695–702.

Wortmann, U.G. & Weissert, H. 2000: Tying platform drowning to perturbations of the global carbon cycle with a $\delta^{13}C_{org}$-curve from the Valanginian of DSDP Site 416. Terra Nova 12, 289–294.

Taxonomic Index